European Research Infrastructure supporting Smart Grid and Smart Energy Systems Research, Technology Development, Validation and Roll Out – Second Edition

Project Acronym: **ERIGrid 2.0**

Project Number: **870620**

Technical Report Lab Access User Project

Innovative RES Solutions for 100% RES System (GRIDPV100)

Access Duration:

6/12/2021-17/12/2021 (remote, Somesh and Chrysanthos)
16/01/2022 – 05/02/2022 (physical, Somesh and Chrysanthos)
21/02/2022 – 25/02/2022 (remote, Chrysanthos)
21/02/2022 – 27/02/2022 (physical, Somesh)

Funding Instrument:	Research and Innovation Action
Call:	H2020-INFRAIA-2019-1
Call Topic:	INFRAIA-01-2018-2019 Integrating Activities for Advanced Communities
Project Start:	1 April 2020
Project Duration:	54 months
User Group Leader:	[Somesh Bhattacharya (MCAST)]

This project has received funding from the European Union's Horizon 2020 research and innovation programme under Grant Agreement No. 870620.

Report Information

Document Administrative Information	
Project Acronym:	ERIGrid 2.0
Project Number:	870620
Access Project Number:	116
Access Project Acronym:	GRIDPV100
Access Project Name:	Innovative RES Solutions for 100% RES Systems
User Group Leader:	Somesh Bhattacharya (Malta College of Arts, Science, and Technology, MCAST)
Document Identifier:	ERIGrid2-Report-Lab-Access-User-Project-AccessGRIDPV100-draft-vn 01
Report Version:	vn.01
Contractual Date:	14/12/2021
Report Submission Date:	01/04/2022
Lead Author(s):	Somesh Bhattacharya (Malta College of Arts, Science, and Technology)
Co-author(s):	Chrysanthos Charalambous (FOSS Research Centre for Sustainable Energy)
Keywords:	[system security, power quality, RES dominant grid], European Union (EU), H2020, Project, ERIGrid 2.0, GA 870620
Status:	Draft

Change Log

Date	Version	Author/Editor	Summary of Changes Made
24/01/2022	v1.0	E. Mrakotsky (AIT)	Draft report template adapted
01/04/2022	v1.1	S. Bhattacharya (MCAST)	Draft report completed
XX/XX/2022	v1.0	C. Charalambous (FOSS)	
XX/XX/2022	v1.0	S. Bhattacharya (MCAST)	

Table of Contents

List of Figures

List of Tables

List of Abbreviations

AIT	Austrian Institute of Technology
AVR	Automatic Voltage Regulator
CCM	Current Control mode
DER	Distributed Energy Resources
DN	Distribution network
DSOGI	Double second order generalized integrator
f-P	frequency-power
HIL	Hardware-in-the-loop
I-V	Current-voltage
LA	Lab access
LV	Low voltage
MPPT	Maximum power point tracker
PV	Photovoltaic
P-V	Power-voltage
PLL	Phase locked loop
RoCoF	Rate of Change of Frequency
SCADA	Supervisory control and data acquisition
SRF	Stationary reference frame
TSW	Transfer switch
UG	User group
UP	User project
VSI	Voltage source inverter

Executive Summary

The Islands of Malta and Cyprus has seen an exponential growth in the uptake of Photovoltaic (PV) technology, especially at the rooftop/ low-voltage (LV) levels. The consolidated uptake, along with the direct and indirect schemes of the governments of the two Islands, is now proceeding fast towards the plan of becoming net-zero emission countries by 2050. The high number of the PV installations in the rooftop levels, however, has seen several problems in the proper operation of the grid, especially during day-time, because of the high PV power produced, and the low-loading at the distribution levels, thereby resulting in voltage rise, however this problem is encountered at a local level. The other problem that is encountered generally on the global level is the frequency regulation problem. The high penetration of PV in a weak system, such as an LV distribution network decreases the effective load, especially during the day time, and the static converters, irrespective of being a source, are essentially constant power loads, therefore, even when there is a frequency variation on the grid side, they keep generating the same amount of power which exacerbates the frequency deviation following load changes or generator events. In order for such converters to participate in the frequency regulation problem, the control loops of such converters need to be redesigned, so that they can participate whenever there is a drop in the load, or when there is an overall frequency change seen from the utility grid side.

The droop control method is a widely used control strategy for frequency regulation within the microgrids, and the same control methodology has also been extended to active distribution networks that can seamlessly enter and exit the islanded mode with the help of a unified control. In the GRIDPV100 project-based lab access at the Austrian Institute of Technology (AIT) in Vienna, we explore the possibilities of PV providing inertial response with the help of the modification of the existing droop control philosophy, and employing a switching-based control that can provide MPPT power in the grid connected mode, and inertial response, when the network goes into the islanded mode. A real Cypriot reduced single feeder distribution network (DN) is used for the studies during this lab access period. Typhoon Hardware-In-The-Loop (HIL) based software is used for creating the simulations to be carried out under a real-time environment to achieve the following goals:

1. Emulate the virtual inertia control for the PV based sources in the distribution network of interest.
2. Compare the performance of the grid-following and grid-forming controls of the PV based on their individual frequency responses.

Preliminary Findings

1. The typhoon HIL based platform gives a deep insight into the grid-forming behaviour of the PV based system. The frequency responses are similar to the droop-controlled battery-based system.
2. The typhoon HIL 604 single arm setup provided to the lab access users did not manage to compile successfully, the simulations for the entire feeder of interest, therefore the reduced model was developed by aggregating the small PVs into a single controllable PV.

Open threads

1. Phasor based location of grid-forming PV in a large distribution network is to be performed
2. Seamless (switching free) control design for the PV based grid-forming converter in the typhoon HIL environment.

1 Lab-Access User Project Information

1.1 Overview

USER PROJECT	
User Project Acronym	GRIDPV100
USER Project Title	Innovative RES Solutions for 100% RES Systems
ERIGrid Reference	116
ERIGRID2.0TA Call	2nd Call
USER GROUP	
Name (Lead)	Somesh Bhattacharya
Organization, Country	Malta College of Arts, Science, and Technology, Malta
Name	Chrysanthos Charalambous
Organization, Country	FOSS Research Centre for Sustainable Energy, University of Cyprus, Cyprus
HOST RESEARCH INFRASTRUCTURE	
Name	AIT Austrian Institute of Technology
Country	Austria
Start and End Dates (Online and 'in-person')	6th December 2021 to 17th December 2021 (Online) 16th January 2022 to 28th January 2022 (In person-Somesh Bhattacharya) 19th January 2022 to 5th February 2022 (In person-Chrysanthos Charalambous) 21st February 2022 to 27th February 2022 (In person-Somesh Bhattacharya) 21st February 2022 to 25th February 2022 (Online-Chrysanthos Charalambous)
Stay and Access days	Somesh Bhattacharya | Stay Days 19 | Access Days 27 Chrysanthos Charalambous | Stay Days 17 | Access Days 27

1.2 Research Motivation, Objectives, and Scope

Research Motivation

Frequency control from the perspective of low voltage distribution network remains an open challenge for the researchers and the power system operators. Active distribution networks are now becoming a reality with more and more PVs and batteries participating in the grid, and also offering grid related services such as voltage and frequency control. Power systems in small Islands such as Malta and Cyprus are different compared to the ones in the mainland. The major difference is the fuel used for the conventional synchronous generators, which are mostly heavy fuel oil or gas oil. Although environmentally friendlier than the coal-based generation, however, the fuel cost for the former is higher. Renewable generation, especially Photovoltaics (PVs) are widespread along both the Islands due to the high insolation, mostly as rooftop plants given the space constraints. However, PVs are inverter-based power sources, which do not provide natural inertial support. This feature is detrimental to the dynamic stability of the power system especially when it comes to non-interconnected or weakly interconnected Islands, and can lead to unacceptable rate of change of frequency (RoCoF), that can lead to power quality issues, generator tripping, unserved load and ultimately total system collapse.

Scopes and Objectives

Proliferation of rooftop PVs raises their stakes to invest in smarter control philosophies. The main idea of this work is to harness virtual inertia from the PVs to obtain inertial response for a typical weak or a non-interconnected grid, in the aegis of a small Island such as Malta or Cyprus respectively. A methodology must be provided to decide, which PV should participate in frequency response, while keeping the controls active for all participating PVs. In principle, it should be the largest capacity PV, which should provide a certain amount of support, however, when all the PVs are of almost the same capacity (especially in Island scenario), the choice becomes more difficult and other technical constraints take place. Therefore, a helicopter view is required to decide, for the set of PVs to work in the grid forming mode, and the rest in the grid following mode.

The main purpose of the lab access is to realize the PV in the distribution network to work in the grid-forming mode, especially once they have entered the islanded mode of operation. The advantages of PV working in the grid-forming mode are manifold, such as lower frequency transients during a load change (E.g. Figure 1 where a load change is simulated and frequency response is observed), and less stress on the battery bank because of the active and the reactive power sharing. It is a known fact that in a distribution network, the PVs cannot participate in any of the market-based operations, and the PV

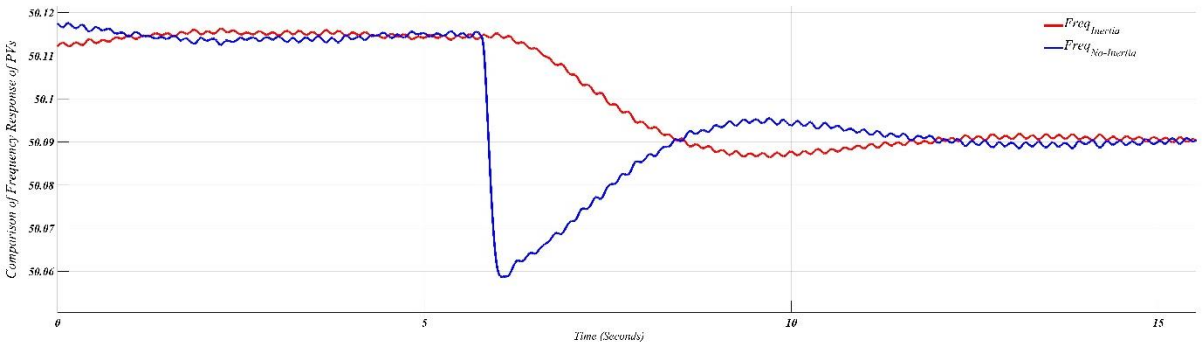

Figure 1: Comparison of Responses of PV with and without inertial control

owner only gets the subsidized rate of the installations, and thereby, de-rating of the PV to some extent will not impact the owner in a negative manner. Therefore, to fulfil the objective of grid-forming PV control, cascaded switching-based controller is designed for the PV in the Typhoon HIL environment, and the studies are carried out on the reduced Cypriote network. The network consists of two aggregated PVs and a utility scale battery, and the latter works in the droop control mode, however, the inertial control isn't embedded as part of the battery controls. To ensure a smooth transition between the grid connected and the islanded modes, a synchronizer is also formulated which ensures a quick transition without any appreciable transients back to the grid-connected mode.

1.3 Structure of the Document

This document is organised as follows: Section 2 briefly outlines the state-of-the-art/state-of-technology that provides the basis of the realised Lab Access (LA) User Project (UP). Section 3 briefly outlines the performed experiments whereas Section 4 summarises the results and conclusions. Potential open issues and suggestions for improvements are discussed in Section 5. Finally, additional information is provided in the Appendix A about the community storage parameters used for the real-time simulations for the network considered.

2 State-of-the-Art/State-of-Technology

Virtual Synchronous Generator (VSG) technology [1] for voltage source inverters (VSI) helps realize ancillary service provision by static generators such as battery-based energy storage systems. However, the only drawback with the VSG technology is that an energy storage system is a primary requirement, in order to serve the demand supply imbalance in a short time interval while also taking care of the rate of change of frequency (RoCoF). This drawback leads to increased use of the storage system for such frequency regulation/ response, and therefore the deterioration of the battery can happen quicker [2].

For the PVs to participate as a VSG or a grid-forming inverter, the source should be allowed to derate itself from the normal maximum power operating point. The normal grid connected PVs, when operating in the off-grid mode require a frequency reference from the diesel generator to continue operating in the off-grid mode. For the PV to operate as a grid-forming inverter, the control strategy is designed in a way, that as soon as a grid outage occurs, the inverter should seamlessly move to the frequency control mode. A grid-forming control approach for PV was demonstrated in [3], where a droop control as responsible for the derating of the PVs in a 9-bus conventional power system. However, the modified controller was realized on a two-stage PV system, i.e. on the DC-DC converter part. This increases the complexity of the controls, and also is not feasible solution for a large PV plant. More related work focused on PV as a VSG was shown in a past literature [4]. This paper reported the PV as a grid-following inverter, while a super-capacitor in conjunction with the PV connected to the same inverter acted as the grid-former. Such methodology is feasible for a smaller number of PVs, however, when we consider a DN at large, the technology akin to the mentioned literature will be a costly solution.

The virtual inertia provision from distributer energy resources (DER) in DNs have been highlighted in a few papers [5], [6]. A flexible power point-based tracking system for the PVs operating within a DN was proposed in [5]. In this work, a reserve margin was held for the PV to supply active power in the wake of an under-frequency event. However, in this paper, islanding conditions were not covered. The operation of PV in an active distribution network, that can deliver virtual inertia and also manage the demand power at the point of common coupling (PCC) by derating the PV power using a consensus-based approach.

The GRIDPV100 focuses on the PV provision of virtual inertia, especially during islanding and reconnection. The grid-forming PV designed in the Typhoon HIL environment can work independently without a battery support. A switching-based controller is designed, i.e. the PV will work in the maximum power point tracking (MPPT) mode while connected to the grid, and become a grid-former in the off-grid mode. The grid-forming PV also includes the synchronization to the utility irrespective of the location of the PV, i.e. even if the PV is not electrically closest to the PCC. Even though a switching controller is used, thanks to the activated virtual inertia control during the synchronization, spurious transients in the active powers and the frequency are not noted, therefore keeping the RoCoF under safe margins. The shaping of the synchronization dynamics was also performed in [2] with the help of the deviation of the DC link voltage into the angle reference, however, this controller was designed considering an absence of a Phase Locked Loop (PLL). This approach considers drooping the DC link voltage as a function of the deviation in frequency, and for a PV working in power sharing with a battery, as the latter DC link voltage remains constant, irrespective of the grid-connection status. Therefore, for power sharing between the PV and the battery in the islanded mode, the frequency-power (*f*-P) droop is used. It is to be noted that for both the PVs and the battery, a double order second order generalized integrator (DSOGI) PLL was used for sensing the angular references to operate in the grid-connected mode. However, this approach does not affect the black-starting capabilities of the sources under test.

3 Executed Tests and Experiments

3.1 Test Plans

The test system considered for the real-time simulations is a single feeder Cypriote network from the real data from a suburban province of Nicosia, as shown in figure 2. The network comprises of an incoming substation with a 11kV/400V transformer, and a community energy storage system, whose specifications are defined in appendix A.

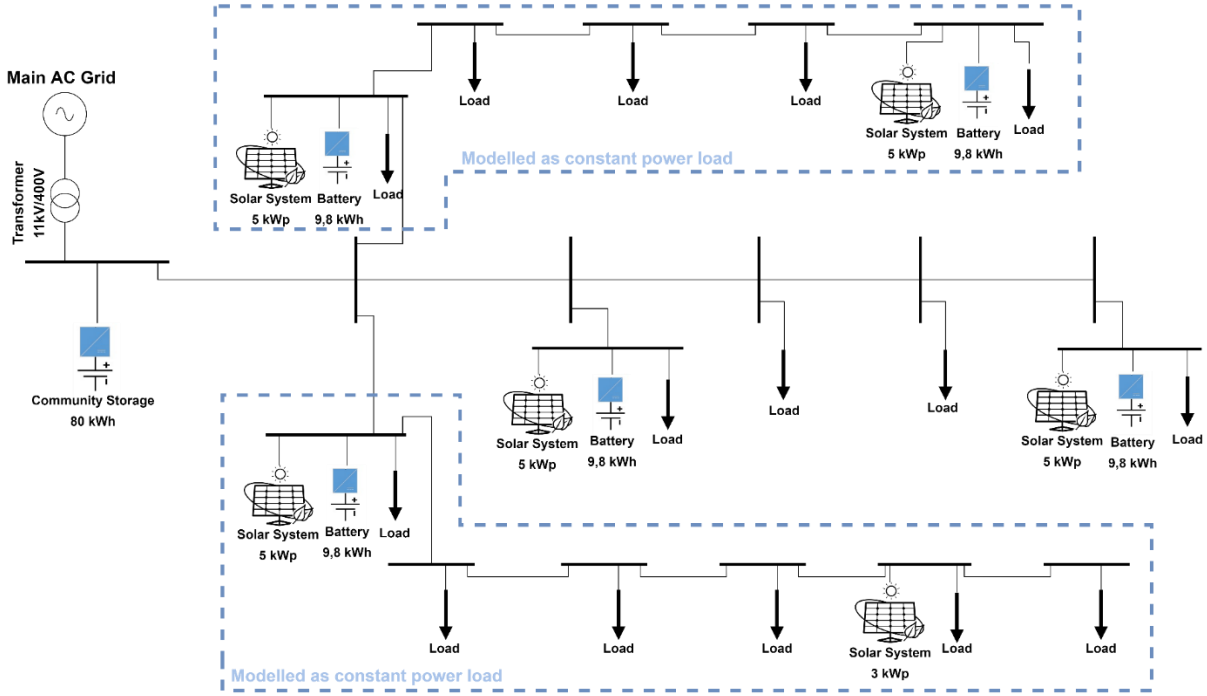

Figure 2: Cypriote Network under Study

The figure shows that two legs of the feeder are modelled as constant power loads. These loads as modelled in the Typhoon HIL platform can be a positive or a negative load, and can have the voltage and frequency droop enabled. The choice of such modelling lies on the fact that the Typhoon HIL 604 processor in the real-time can generate signal processing errors if the network is modelled with switching VSIs in all entirety. The other loads shown in the figure are constant impedance loads.

3.1.1 Testing plans on the network

The initial days of the lab access carried out in December 2021 (online) and January 2022 (in-person) focused on the development of the network, and testing the controls on a reduced network comprising of a single PV with 22kW rating with MPPT voltage around 800V-DC at one bus, and a battery as a DC source at another bus. The purpose of this test was to corroborate the controls developed (details in section 3.2.1). The real-time simulations on the aforementioned network were carried out with the help of Typhoon HIL 402 setup. The tests on the Cypriote network were held after verification of the results for the reduced network. The summary for the testing plans and implementations is shown in Table 1.

Table 1: Tests performed

Dates	*Activity*
6th December (online)	Introduction between the user group and the AIT host members
7th December to 10th December (online)	User group skill uptake on the Typhoon HIL platform using remote desktop provided by AIT and downloading the free version of Typhoon Virtual HIL.
13th December to 17th December (online)	Study of the droop-controlled battery based VSI operating in both grid-connected and islanded modes using Typhoon HIL
17th January to 19th January (in-person/ UG leader)	Development of the reduced network with PV and battery using the Typhoon HIL 402 setup
20th January (in-person)	Kick-off meeting and development of the work plan for the rest of the lab access
20th January to 28th January	Real-time simulations on the reduced network and the development of the Cypriote network
21st February to 24th February (in-person/ UG leader)	Real-time simulations carried out for various scenarios using the Typhoon 604 setup: • MPPT operation of the PV (grid-following mode) while keeping the battery in the droop control mode • Virtual inertia (grid-forming mode) testing of the PV working in tandem with the battery for the network. • Scenarios developed, such as grid-connected to islanded, black-start of PV without battery, islanded to grid-connected (Synchronization control tested).
25th February (in-person/ UG leader)	Recording of the results for the various scenarios tested.

3.2 Test Set-up

The tests are performed on a Cypriote distribution network with real data with two aggregated PVs. The term aggregated PVs comes from the fact that as there are several PVs of smaller capacities, in between 5kW and 9kW, the inverter controls are aggregated into a single controller for the ease of implementation, and to implicate lesser burden on the single arm processor of the HIL 604. The aggregated PVs are culminated into two PVs 22kW each. The Power-Voltage (P-V) and Current-Voltage (I-V) curves for the same can be seen in figure 3. The community battery energy storage, that is closest to the PCC is rated at 90kWh, that is connected to a VSI with 35kW nominal power rating.

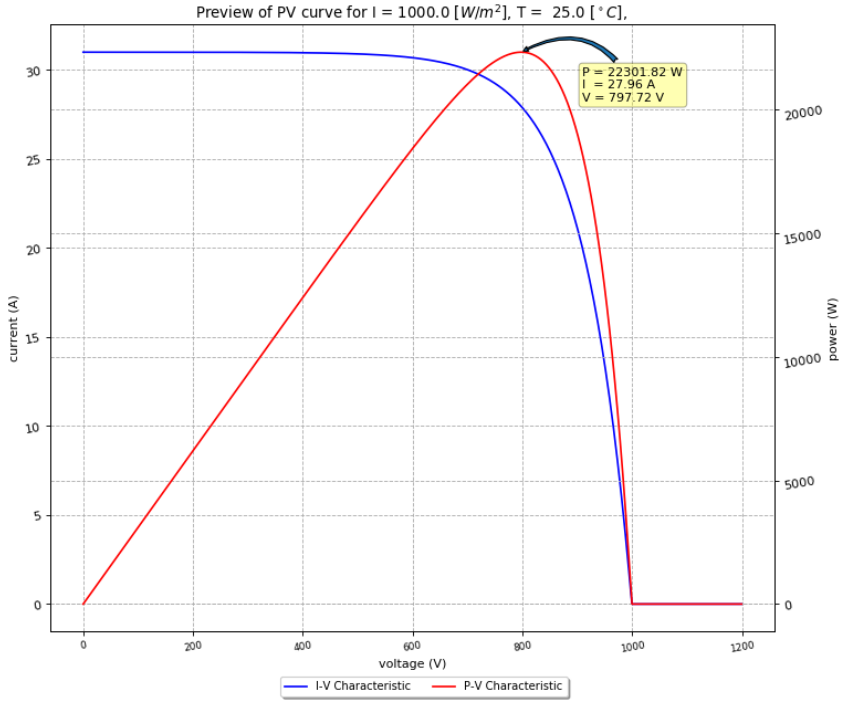

Figure 3: P-V and I-V Curves for the aggregated single PV

3.2.1 Virtual Inertia Based Switching Control for PV

The switching control strategy is discussed further in this section. The PV control is so designed that the same can work in both current control mode (CCM) and the voltage control mode (VCM). The VSG capability of the PV is realized once it is in the islanded mode, i.e. working as a VCM. While working under CCM, normal MPPT operation is realized.

The control structure for the VSI as a single-stage PV is designed to be cascaded, with the outer loop being the inertial control, whereas the inner control loops being the voltage and the current controllers. The design of the outer loop inertial controller comes from the fact that the DC link capacitor can release potential energy, that is equivalent to the kinetic energy released during a power imbalance in a conventional power system, the dynamics of which is governed by the popular swing equation, as described in per units (p.u.) in (1).

$$P_m - P_e = 2H.\frac{d\Delta\omega}{dt} \quad (1)$$

In the equation, P_m and P_e denote the mechanical and the electrical powers respectively. *H* is

the inertia constant in seconds, and ω is the PV generated frequency in radians per seconds. The inertia constant is calculated by equating the energy equations for the DC link capacitor and the kinetic energy stored in the rotor of the synchronous machine. The expression for the inertia constant can be seen in (2).

$$H = K_{\omega}.\frac{C_{dc}.V_{dc0}.\omega_0}{2.VA_{base}} \quad (2)$$

The control diagram for the Pulse Width Modulation (PWM) control of the VSI can be seen in figure 4.

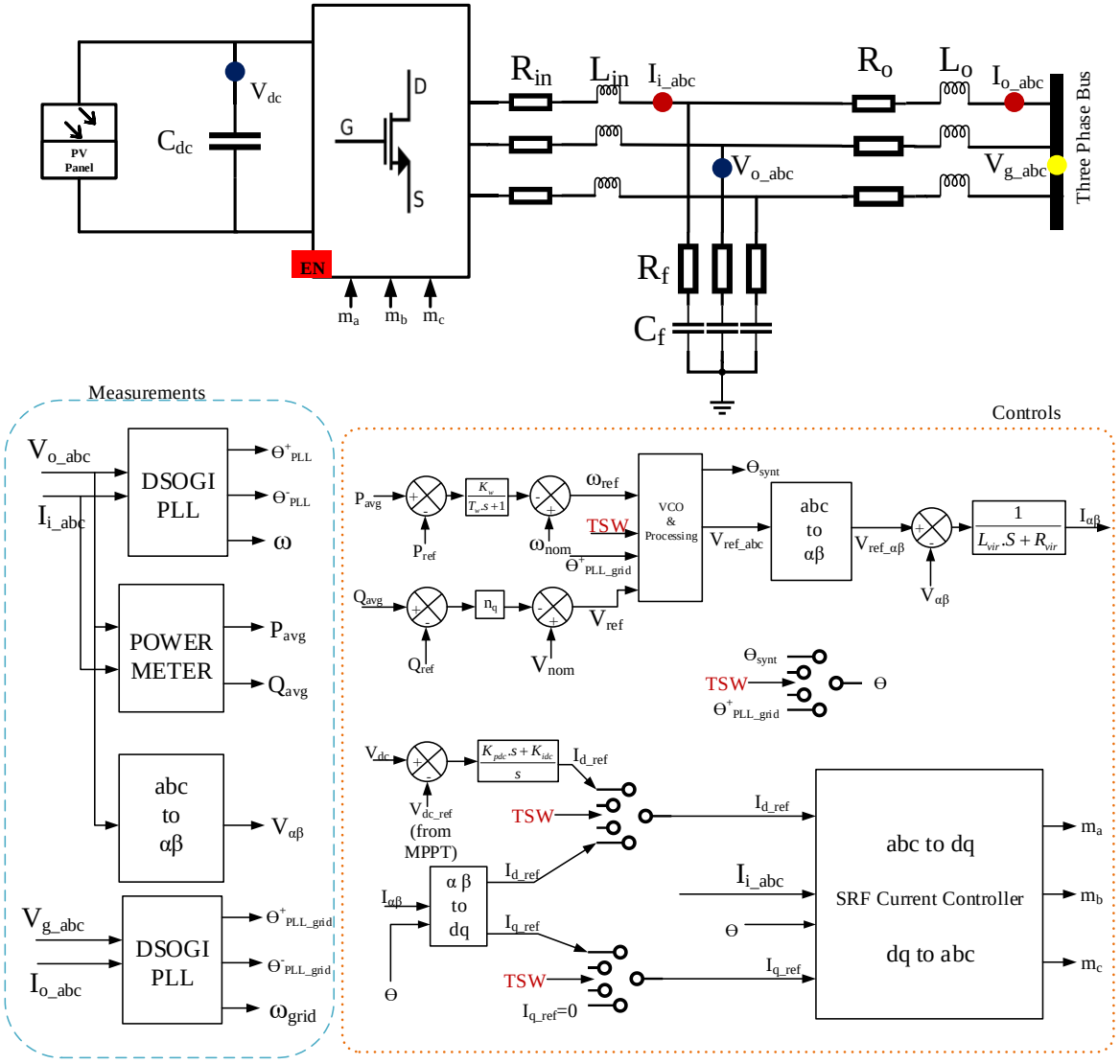

Figure 4: Control Strategy for PV as a grid-forming inverter

The control approach for the PV as a grid-forming inverter, as seen in figure 3 is modelled as a switching controller. In the figure, an LC filter is used for the attenuation of the harmonic order frequency components. The output current and the voltage is sensed as I_{i_abc} and V_{o_abc} respectively. The grid currents and the voltages are sensed as I_{o_abc} and V_{g_abc} respectively. The DSOGI PLL [7] then is used for the estimation of the positive and negative phase angles (Θ^{+}_{PLL} and Θ^{-}_{PLL}), along with the system frequency, ω.

The grid-forming control is realized by generating the frequency and the voltage references

assisted by the virtual inertia and the droop-based voltage control. The latter control generates the voltage reference as a function of the reactive power requirements by the loads. This control is a mimic of the automatic voltage regulator (AVR) of the conventional synchronous generator. The equation for the virtual inertia control, and the voltage droop as implemented in the typhoon HIL software can be summarized in (3) and (4):

$$\omega_{ref} = \omega_{nom} - \frac{k_w}{T_w.s+1}(\mathrm{P}_{avg} - \mathrm{P}_{ref}) \quad (3)$$

$$V_{ref} = V_{nom} - n_q(Q_{avg} - Q_{ref}) \quad (4)$$

In the equations above, the parameters ω_{ref} and ω_{nom} are the generated frequency reference, and the nominal frequency set at 100π radians per seconds (or 1 p.u.) respectively. The reference and the calculated average powers are P_{ref} and P_{avg}. K_w is the droop coefficient, while the time constant Tw is H/D, where D is the damping coefficient. The inner voltage and current controllers are based on virtual admittance and the decoupled Synchronous reference frame (SRF) based controllers. The firing pulses are thus generated through the SRF control. The modulation index, m_{abc} is then fed to the VSI. EN (1/0) in the figure is the *enable* option for the inverter which can be triggered through the supervisory control and data acquisition system (SCADA).

The battery control is developed in the exact same lines as the PV, except the switching controller. Therefore, the battery continues to work in the *f*-P droop control mode irrespective of the grid connection status. The figure for the same is not shown for the sake of brevity.

Synchronization with the Utility Grid

The utility grid synchronization of the PV and the battery VSIs is achieved with the help of a transfer switch (TSW), that has 1/0 output. The difference between the instantaneous grid voltage (V_{g_abc}) and the VSI output voltage is measured, and if the difference is less than 10, the comparator switch is set to 'high' position, and if the TSW value is '1', then the comparator signals the utility transfer switch to close, thus connecting the grid with the active distribution network. The switch is automatically turned off as soon as one of the two conditions are violated. This logic can be seen in figure 5.

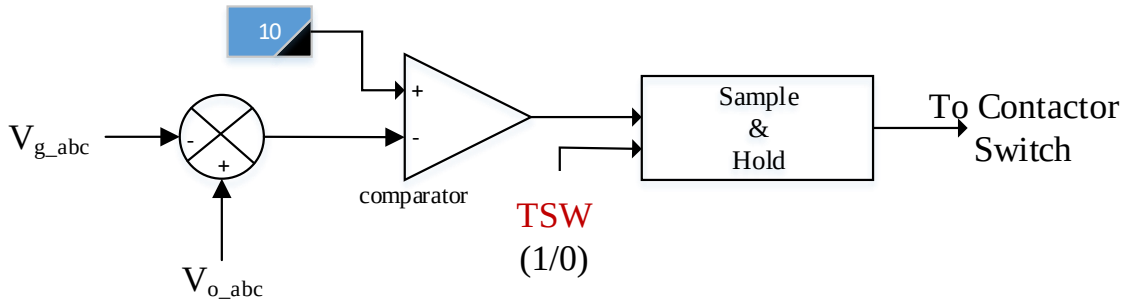

Figure 5: Synchronization logic

3.2.2 Typhoon HIL SCADA

The Typhoon HIL SCADA is used to visualize the results of the setup. The SCADA inputs help in changing the relevant controller gains and PV irradiance in real-time, while the capture settings of the scope help in visualizing the instantaneous responses of the voltages, currents, and the phase angles in accord with the user choices. For the real-time simulations carried out

at AIT, the SCADA inputs of interest can be tabulated below in Table 2, and a snapshot of the SCADA can be seen in figure 6.

Table 2: SCADA input parameters for the system considered

SCADA Inputs	*Values*	*Comments*
Energy Storage and PV(s) Enable (EN)	1/0	'1' will enable the VSI. '0' disables the VSI and controls but stays connected to the system.
Energy Storage and PV(s) V_{ref}	1	Always set to 1
Energy Storage and PV(s) ω_{ref}	1	Always set to 1
Energy Storage and PV(s) P_{ref}	0	Ranging between 0 and 1 (measured in p.u.)
Energy Storage and PV(s) Q_{ref}	0	Ranging between -0.2 and 0.2 (measured in p.u.)
Energy Storage and PV K_p (SRF Current Controller)	2	May vary depending upon the filter and simulation time step
Energy Storage and PV K_i (SRF Current Controller)	0.25	May vary depending upon the filter and simulation time step
PV(s) K_{pdc} and K_{idc}	1.5/150	May vary depending upon filter (capacitor value)
PV(s) Irradiance	200-1000	Varied according to the case requirements
Transfer switch (TSW)	1/0	According to grid conditions (ON/OFF)

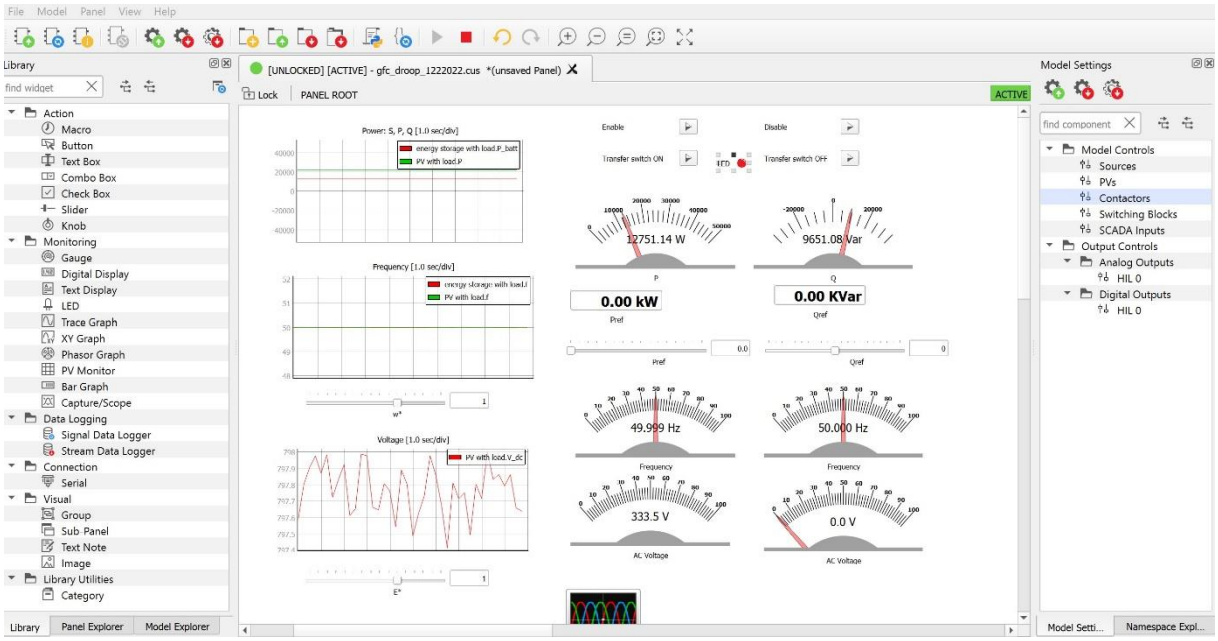

Figure 6: Typhoon HIL SCADA Snapshot

3.3 Data Management and Processing

The data requirements pre-simulations for the GRIDPV100 project were low. The Cypriote network data was already provided to the lab access user from Cyprus. During the simulations, the data requirement was minimal, as the real-time simulations carried out using the Typhoon HIL 402 and 604 were dependent on the ratings of the VSI and the line and the load data obtained for the Cypriote network. The data that was generated from the simulations were both instantaneous type data and the steady state type data. The instantaneous data such as the grid voltage, PV voltage and the energy storage voltage, and the Phase angles were plotted directly from the Typhoon HIL SCADA, and the quasi steady state data such as frequency, active powers, and the DC link voltage of the PV and storage were exported as a *csv* file to excel, and later plotted using the 'plot' tool of MATLAB.

4 Results and Conclusions

4.1 Discussion of Results

This section summarizes the results obtained for the lab access duration of the GRIDPV100 project. The results were obtained keeping the execution rate at 100µsec. The reduced model was built using 50 µsec, however, in the actual network model, this rate caused the system CPU to stall (more information in section V), and thereby the choice of 100µsec was made. The results that were obtained for the various scenarios are deliberated in the following sub-sections.

4.1.1 Black-Starting Capability

This section describes the black-starting capability of the sources in the network, i.e. the battery and the two aggregated PVs. This condition is realized in the Typhoon HIL simulations by setting the TSW to 0, thus switching the contactor to the grid to 'OFF'. The network thus operates in the islanded mode.

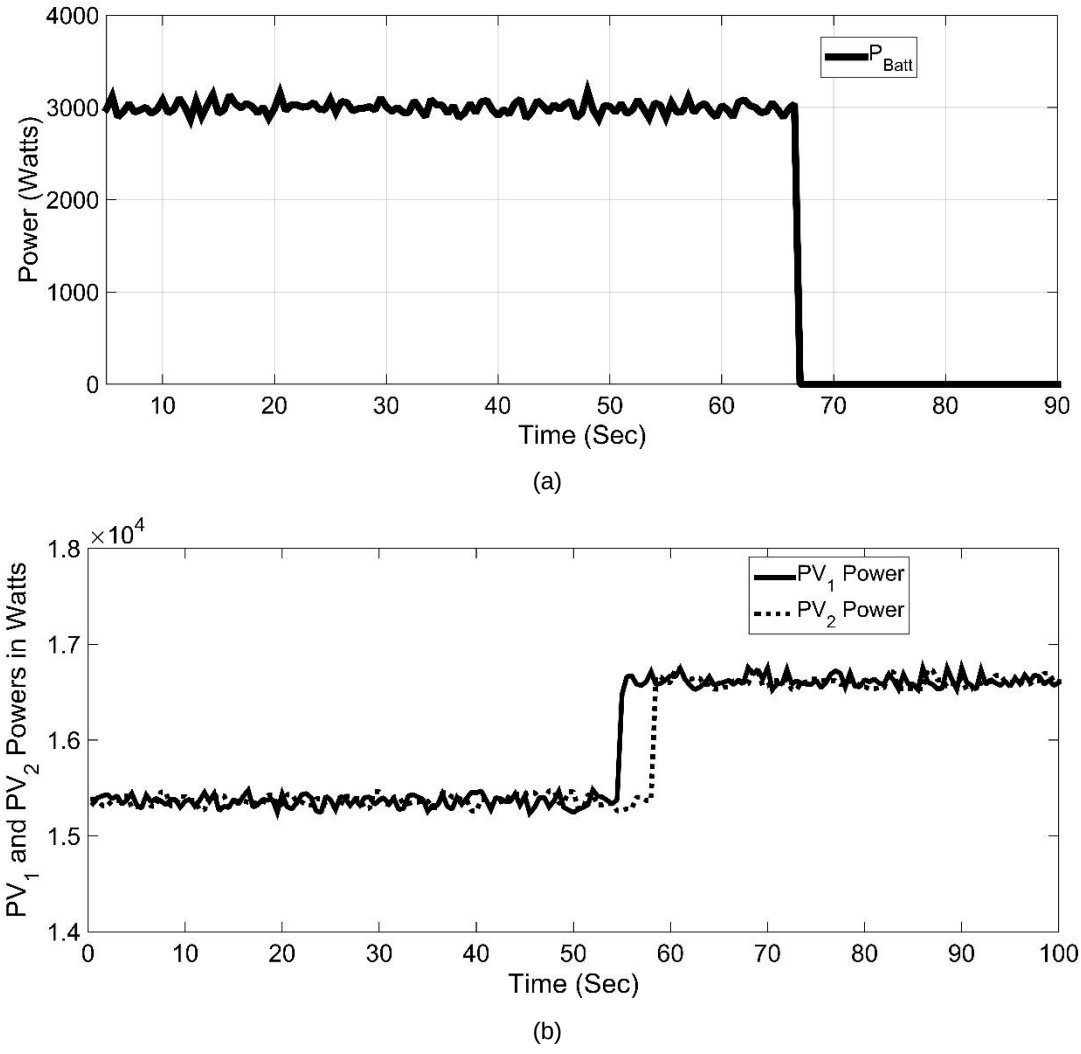

Figure 7: Measured Active power during black-start for (a)Battery and (b)PVs

Figure 7 shows the responses of the battery storage and PV when the operation starts in an islanded mode. This response is typical of a day time with 100% irradiance available. The total connected load in the islanded part of the network is 23kW, excluding the part that is modelled as a constant power load (CPL). It is assumed that at the point of connection (POC) of the two CPLs, the total incoming active power is 11kW. Thus, with the same droop coefficient, K_w of 2% the PVs and 5% for the battery, and 'H' kept at 15%, the powers shared are 15.5kW each for the PV, and 3kW for the battery. The scenario considered within the simulations is that of the cessation of the battery power, i.e., it reaches less than the permissible SoC for operation, thus, the PVs take up the change in the power. The measured frequency from the DSOGI-PLL for one of the PVs and the battery is shown in figure 8.

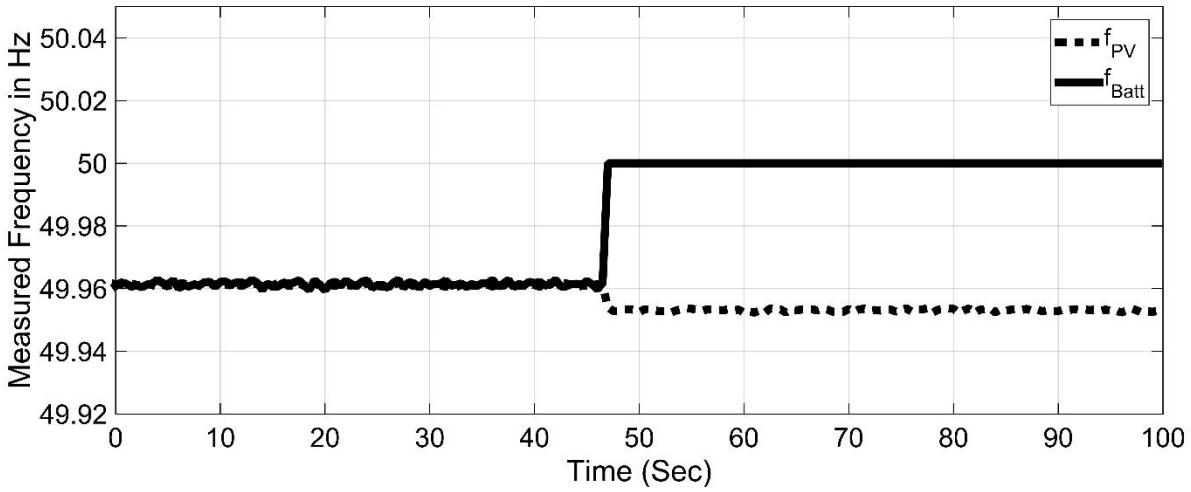

Figure 8: Measured frequencies during black-start for PVs and battery

4.1.2 Grid Connected to Islanded Operation

This section describes the operation of the network, entering the islanded mode from the grid-connected operation. The responses of the PVs and the batteries and the measured frequencies are shown below in figures 9 and 10.

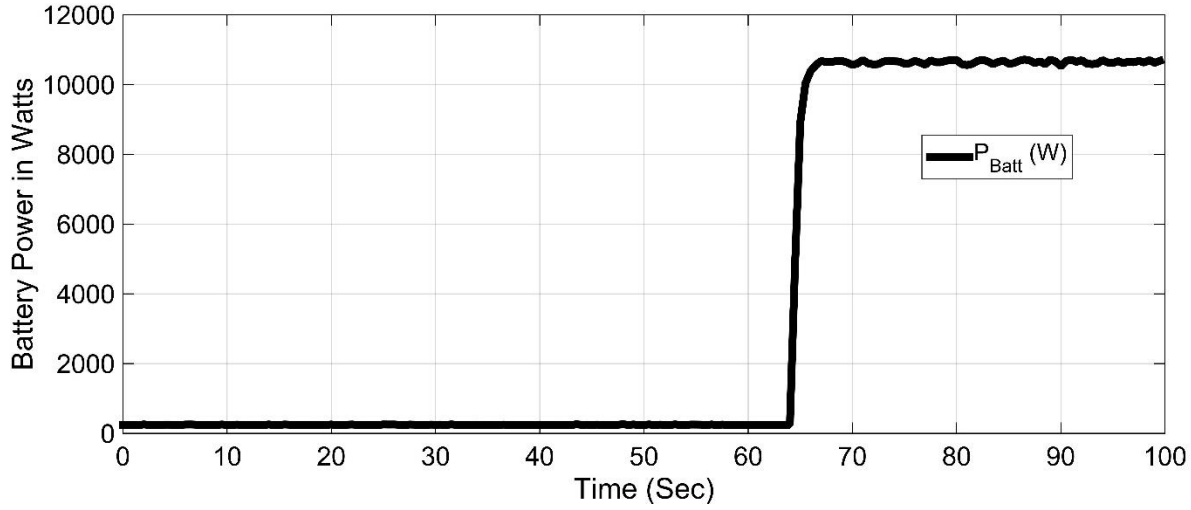

(a)

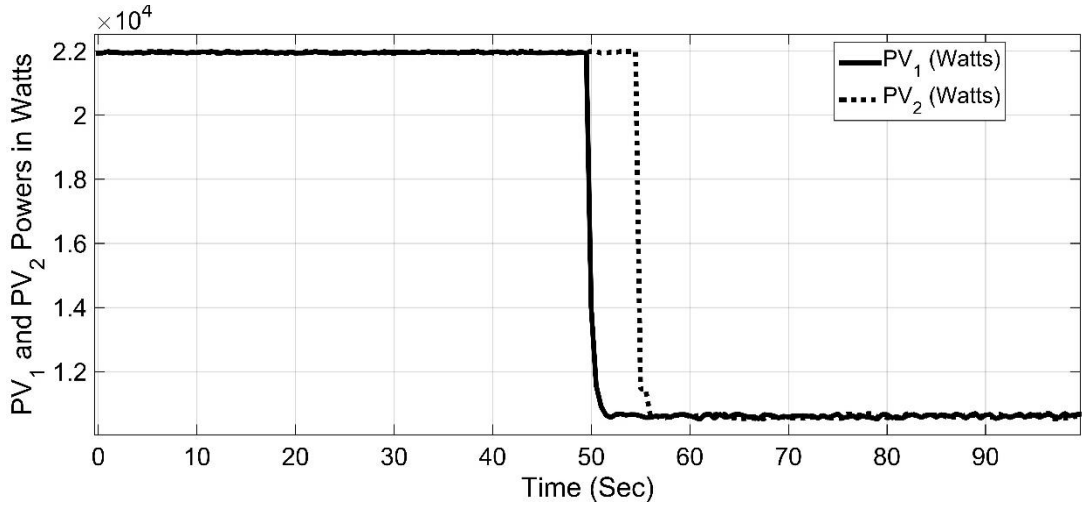

(b)

Figure 9: Grid to Islanded mode power measurements for (a) Battery (b) PVs

The above Figure 9 shows the transition of the PVs and batteries from the grid-connected mode to the islanded mode. It is observed that initially, the PVs operate at their MPPT, while the batteries are considered to be floating with the P_{ref} set to 0. However, as soon as the network enters the islanded mode, all the sources share powers in accord with the droop coefficient, K_w. It is also observed that there are no transients during the transition, even in the presence of a switching-based controller. The measured PV frequency can be seen in figure 10.

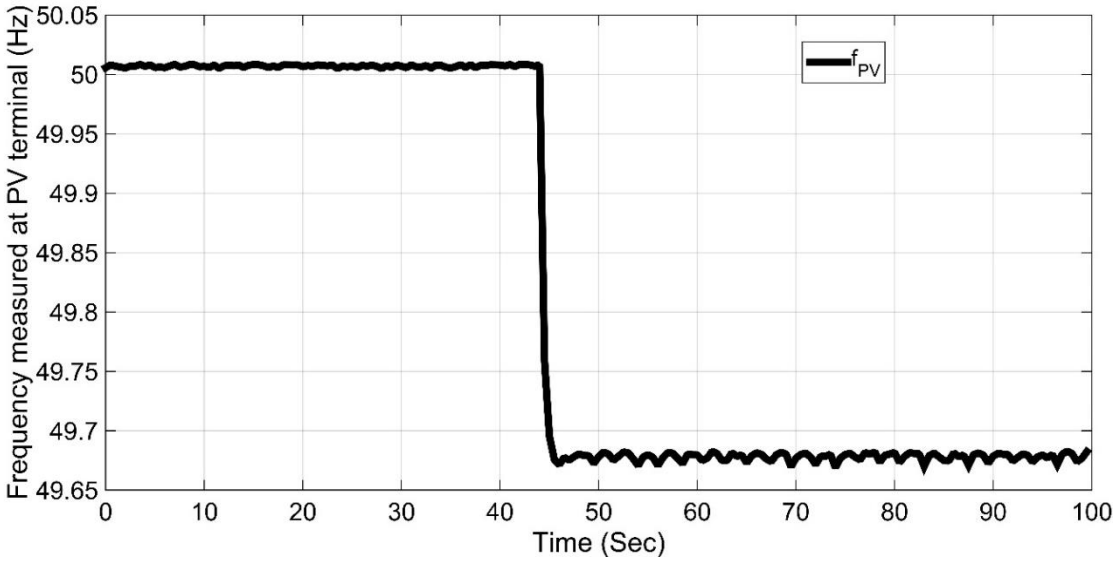

Figure 10: Grid-connected to islanded mode Frequency measured at PV terminal

The instantaneous Battery and the PV voltages in the islanded mode, and the visible phase difference between the grid 'Θ' (measured at the PCC) and the local VSI 'Θ' (measured at the battery VSI point) is shown in figure 11. It can be seen in this figure that the voltage is 326V, i.e. the peak phase voltage, which is measured locally at the PV and the storage.

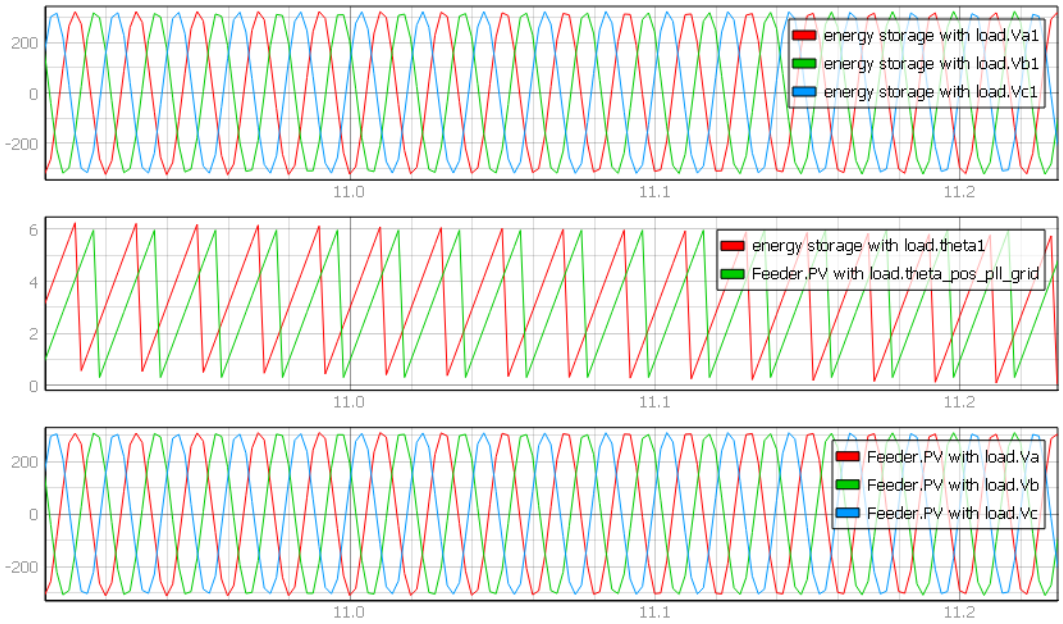

Figure 11: Grid connected to Islanded mode Instantaneous Phase Voltages Battery and PV, and the phase difference

4.1.3 Islanded to Grid-Connected Mode

The Islanded to the grid-connected operation of the sources, i.e. the two aggregated PVs and the community storage with the synchronization to the grid is described in this section. Figure 12 shows the plots for battery storage active powers, as the network enters the grid-connected mode.

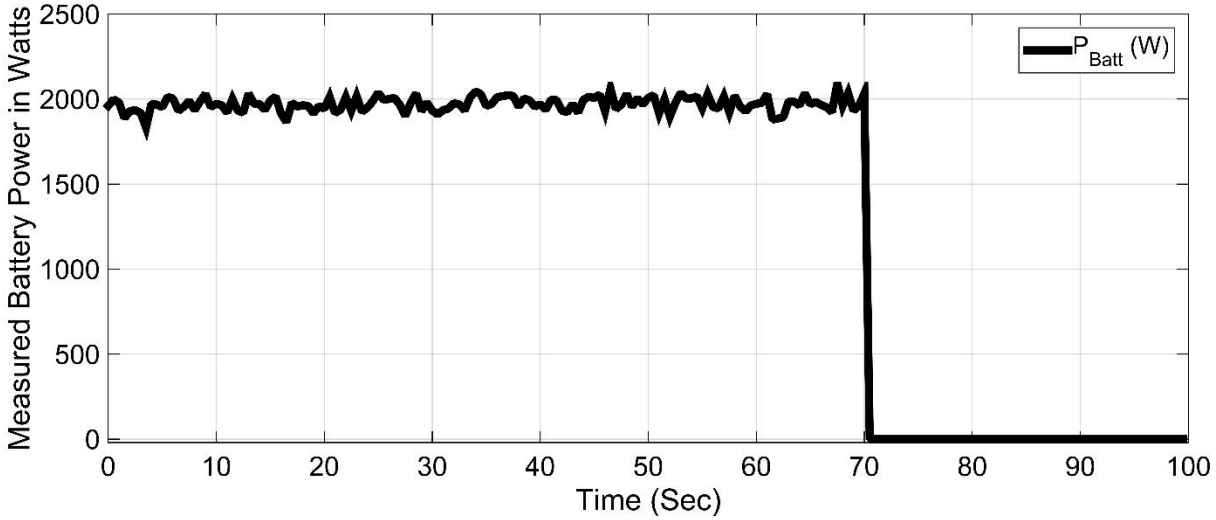

(a)

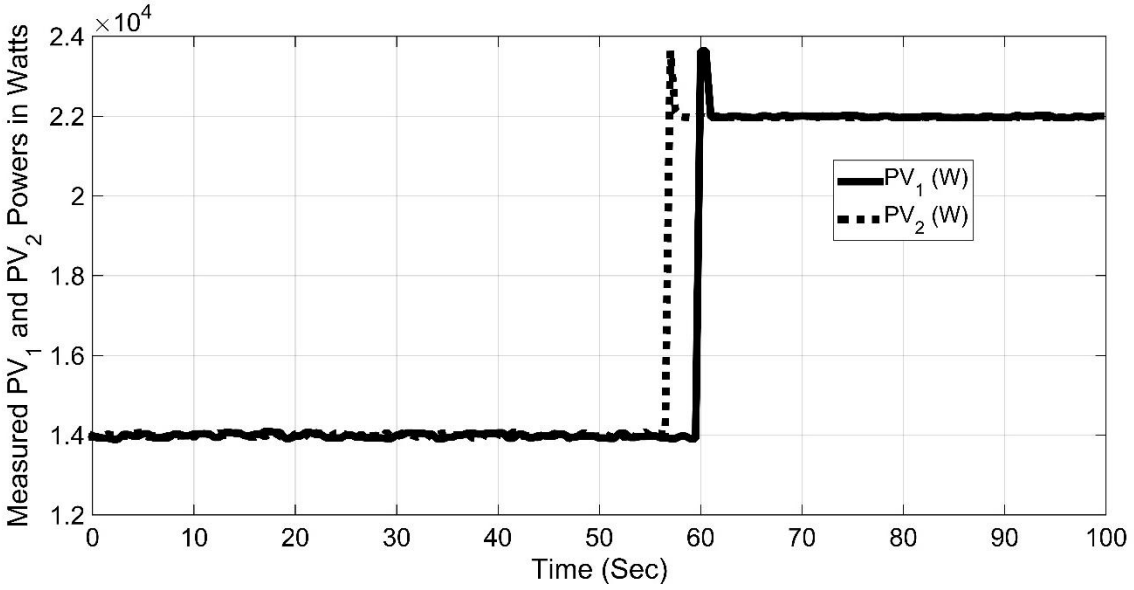

(b)

Figure 12: Islanded to grid-connected mode Measured Active Power of (a) Battery (b) PVs

The figures above show a smooth transition of the active powers from islanded to the grid connected mode. Minor transients are observed in the PV powers during the aforementioned transition. It is observed that the PVs retain their MPPT position, as soon as they enter the grid-connected mode, and the battery also retains its initial '$P_{ref}=0$' position. The plots for the frequency, and the instantaneous measurements (voltage and phase angles) are shown in figures 13 and 14 respectively, for the synchronization scenario.

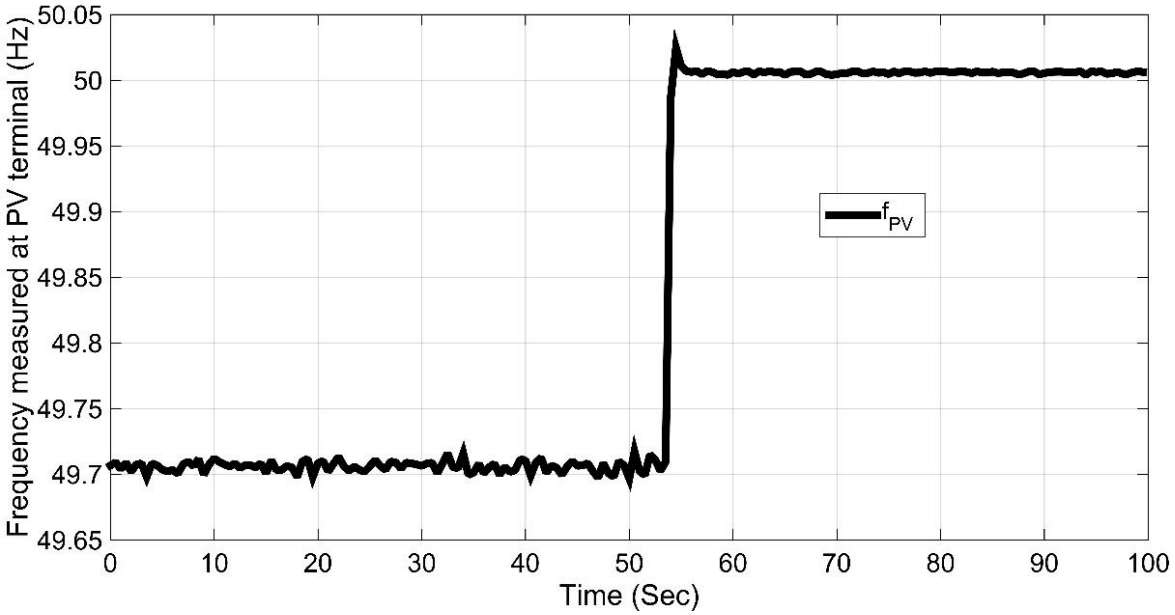

Figure 13: Islanded to grid-connected mode Frequency measured at the PV terminal

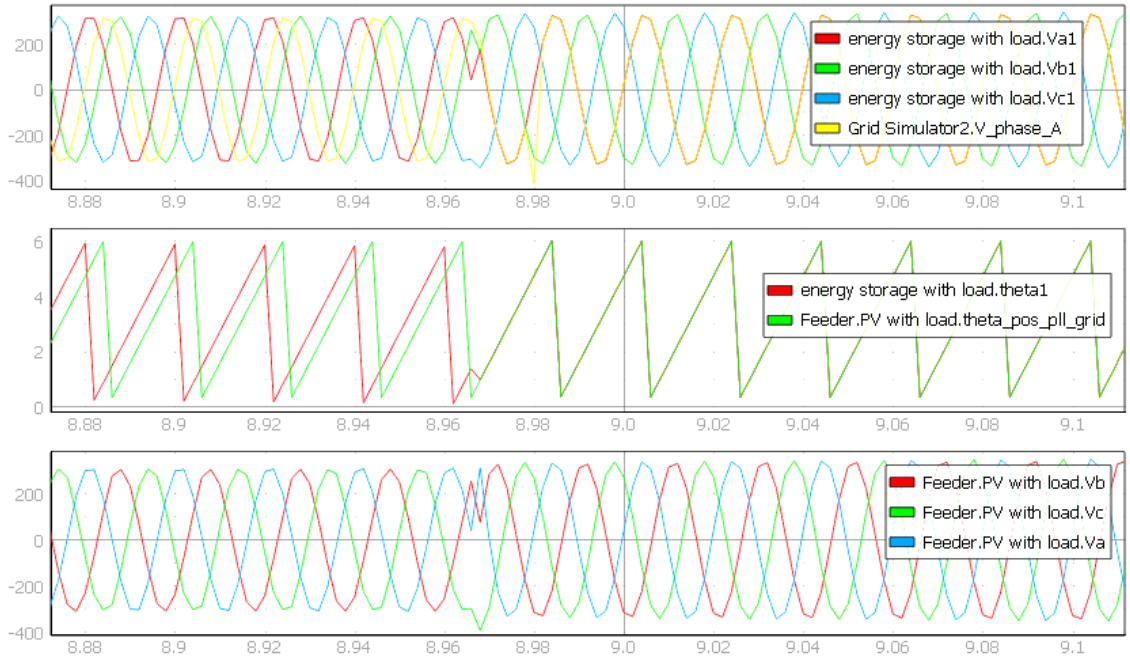

Figure 14: Islanded to grid-connected mode Instantaneous Voltages and phase angles

4.2 Conclusions

The GRIDPV100 project focused on the grid-forming capability of the PV, that can seamlessly work in both grid-connected and islanded modes of operation, and the synchronizer enables a transient free switching for the PVs and the energy storage to reconnect to the grid. The designed grid-forming based switching controls for the PV were tested on a Cypriote distribution feeder network using Typhoon HIL 604 based real-time simulations. Satisfactory results were obtained when several low-rating PVs were aggregated into a single PV for the ease of implementation. The main findings under the lab access were:

1. When all the PVs operate in the grid-forming mode, especially in the islanded operation, the system reliability is enhanced, as frequency and voltage deviations from their nominal values is low, and load changes within the network are catered to by all the sources.
2. Virtual inertia-based design of the outer controller for the PV helps in transient-free load change, which helps in maintaining the RoCoF to the minimum value.

The project implemented under the TA as the UG implements only the grid-forming VSI for PV, which forms the basis for further studies, which can be taken up as part of submission of further calls from the UG. These comprise of the following:

1. Developing a holistic control for the grid-forming PV, that can provide both frequency and voltage-based services, which essentially includes low voltage ride through capability in both modes of operation, as the grid-forming VSI can operate in the derated power range, thereby providing headroom for the reactive power, in accord with the reactive power capability of the PV inverter.
2. A phasor-based determination of the optimal location of the grid-forming PV in a large distribution network.

5 Open Issues and Suggestions for Improvements

The implementation of the GRIDPV100 project involved the use of the Typhoon HIL 604 processor. However, the challenges that were met, together with the unresolved ones are seen in table 3.

Table 3: Status of the real-time simulations GRIDPV100

Issue	*Status*	*Comments*
Use of the entire Cypriote network with average model of PVs and batteries, including the controlled VSIs for the real-time simulations	Unresolved	The entire network could not be simulated because of the arithmetic overflow error. The controller was in the user CPU that was overloaded, and the system CPU had significant free space to accommodate the controllers. However, the transfer of the controller processing to the system CPU could not be performed.
Accurate partitioning of the network thus incorrect monitoring of the system frequency (not faced in the reduced microgrid mimic model) thus causing very high frequency chattering and offset of 0.005Hz in the grid-connected mode	Partially resolved	Core couplings (CC) were placed for all the droop/ virtual inertia controlled VSIs, the determination of the proper choice of the value of the CC inductance however was a challenge.

References

[1] J. Driesen and K. Visscher, “Virtual Synchronous Generators,” *In Proc. IEEE PES General Meeting*, PA, USA, 2008, pp. 1-3.

[2] Y. Qi, H. Deng, X. Liu, and Y. Tang, “Synthetic Inertia Control of the Grid-Connected Inverter Considering the Synchronization Dynamics,” *IEEE Transactions on Power Electronics*, Vol.37, No.2, pp. 1411-1421, February 2022

[3] B. Pawar, E.l. Batzelis, S. Chakrabarti, and B.C. Pal, “Grid-Forming Control of PV Systems with Power Reserves,” *IEEE Transactions on Sustainable Energy*, Vol.12, No.4, pp. 1947-1959, October 2021

[4] X. Quan, R. Yu, X. Zhao, Y. Lei, T. Chen, C. Li, and A.Q. Huang, “Photovoltaic Synchronous Generator: Architecture and Control Strategy for a Grid-Forming PV Energy System,” *IEEE Journal of Emerging and Selected Topics in Power Electronics*, Vol. 8, No.2, pp. 936-948, June 2020

[5] H.D. Tafti, G. Konstantinou, J.E. Fletcher, L. Callegaro, G.G. Farivar, and J. Pou, “Control of Distributed Photovoltaic Inverters for Frequency Support and System Recovery,” *IEEE Transactions on Power Electronics*, Vol. 37, No.4, pp. 4742-4750, April 2022

[6] S. Fahad, A. Goudarzi, and J. Xiang, “Demand Management of Active Distribution Network Using Coordination of Virtual Synchronous Generators,” *IEEE Transactions on Sustainable Energy*, Vol. 12, No. 1, pp. 250-261, January 2021

[7] A.A. Nazib, D.G. Holmes, and B.P. McGrath, “Decoupled DSOGI-PLL for Improved Three Phase Grid Synchronization,” *In Proc. 2018 International Power Electronics Conference*, Japan, 2018, pp. 3670-3677

Appendix A. Community Energy Storage Data

The table 4 as part of the appendix shows the battery parameters for the community energy storage used in the Typhoon HIL based real-time simulations.

Table 4: Battery parameters

Battery inverter	
Power rate	30 KW / 30 KVar
Efficiency	97%
Relative humidity range	5% to 95%
Nominal grid voltage	3PH: 400VAC ± 10%
Communication with battery	Modbus TCP/IP
Ingress Protection (IP) rate	IP21
DC input voltage range	100V – 500V / 360V
Installation	Indoor
Battery Unit	
Technology	Lithium Nickel Manganese Cobalt Oxide
Voltage Range	384V to 498V
Relative humidity range	5% to 95%
Installed battery unit capacity	Nominal: 80 kWh Usable: 50 kWh
Depth of Discharge (DoD)	95%
Communication with the inverter	CAN bus
Ingress protection (IP) rate	IP21
Operating Temperature Range	5^{o}C to 35^{o}C
Installation	Indoor

Disclaimer

This document contains material, which is copyrighted by the authors and may not be reproduced or copied without permission.

The commercial use of any information in this document may require a licence from the proprietor of that information.

Neither the Lab Access User Group as a whole, nor any single person warrant that the information contained in this document is capable of use, nor that the use of such information is free from risk. Neither the Lab Access User Group as a whole, nor any single person accepts any liability for loss or damage suffered by any person using the information.

This document does not represent the opinion of the European Community, and the European Community is not responsible for any use that might be made of its content.

Copyright Notice

This project has received funding from the European Union's Horizon 2020 research and innovation programme under Grant Agreement No. 870620.